# Global Optimization of Cerebral Cortex Layout

*Supplementary Online Material*

Christopher Cherniak*, Zekeria Mokhtarzada,
Raul Rodriguez-Esteban, B. K. Changizi

Functional areas of mammalian cerebral cortex seem positioned to minimize finely costs of their interconnections, down to a best-in-a-billion optimality level. Macaque and cat cortex rank better in connection optimization than the wiring of comparably structured computer chips, but somewhat worse than the economic commodity-flow network among U.S. states. Cortex wiring conforms to a Size Law better than the macroeconomic patterns, which may indicate cortex optimizing mechanisms involve more global processes.

## Conclusion



* To whom correspondence should be addressed:

Committee for Philosophy and the Sciences, Department of Philosophy, University of Maryland, College Park, MD 20742, USA. cc27[at]wam[dot]umd[dot]edu

Next

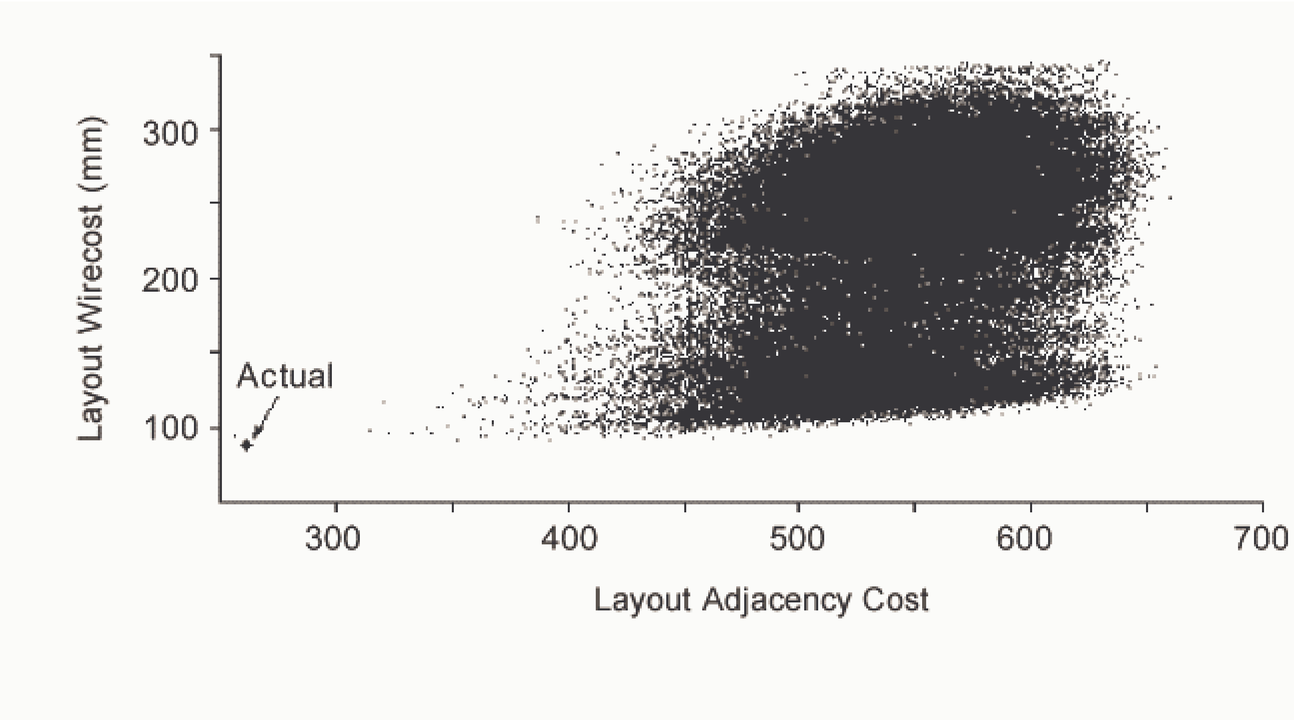


Enlarge

**Fig. S1** . Adjacency rule conformance, vs total wirecost, of 100,000 C. elegans ganglion layouts randomly sampled from the set of all 11! possible layouts.(1) Adjacency rule: If two components are connected, then they are adjacent to each other.(1) A layout is scored in terms of its number of violations of this "all or nothing" adjacency rule. Correlation between good adjacency rule performance and cheap wirecost is not strong ($r^2 = 0.05$); generally, the adjacency rule is not an effective means to good wirecost. However, the small set of nematode nervous system layouts best fitting the adjacency rule--the points at the far left--behave markedly differently: they correspond closely to the best wirecost layouts. (The larger point at the far left of the dispersion diagram represents the actual, minimum-wirecost layout.) Thus, good adjacency rule scores are worth exploring as a surrogate for wirecost of layouts.

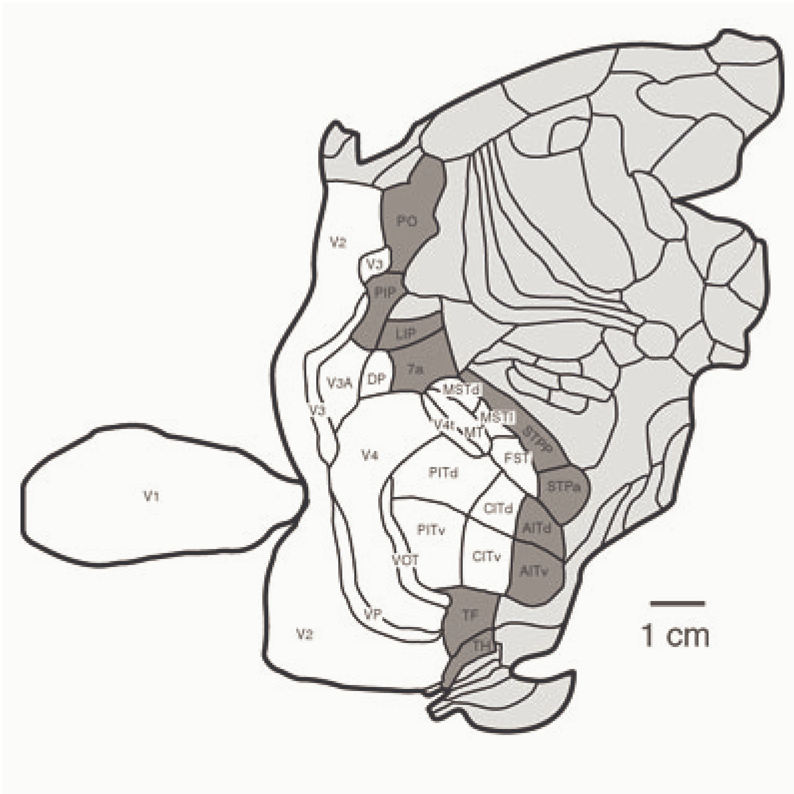


**Fig. S2** . Parcellation of cerebral cortex of macaque. Connection-cost optimization analysis of layout of 17 core areas of the visual cortex (white), along with 10 immediately contiguous "edge" areas (dark gray): Placement of the interconnected functional areas is evaluated for how well total interconnection costs are minimized. 120 connections are reported among the core areas and with the edge areas. Core and edge areas are listed in Table S1 connection matrix below. Rostral is to right.(2)

**Table S1** . Combined connection and adjacency matrix for macaque visual cortex. The series of 17 core visual areas shown above in Fig. S2 is listed (V1 - CITv), in the order in which the areas successively added to the analysis. They are followed by the set of 10 edge areas for the total core (PO - TH). Connections of an area to itself are excluded. A cell with 0 indicates no known connection between the area of that row and of that column; 1 indicates connection in one direction between the two areas; 2 indicates two-way connection. Cell values in **bold** designate topological contiguity of the two areas on the cortex sheet, as in Fig. S2.(3)

| | V1 | V2 | V3 | VP | V3a | V4 | DP | VOT | V4t | MT | MSTd | MSTl | FST | PITd | PITv | CITd | CITv |
|---|---|---|---|---|---|---|---|---|---|---|---|---|---|---|---|---|---|
| V2 | **2** | | | | | | | | | | | | | | | | |
| V3 | 2 | **2** | | | | | | | | | | | | | | | |
| VP | 0 | **2** | 1 | | | | | | | | | | | | | | |
| V3a | 2 | 2 | **2** | 2 | | | | | | | | | | | | | |
| V4 | 2 | **2** | **2** | **2** | **2** | | | | | | | | | | | | |
| DP | 0 | 0 | 0 | 0 | **2** | **2** | | | | | | | | | | | |
| VOT | 0 | 2 | 0 | 2 | 0 | **1** | 0 | | | | | | | | | | |
| V4t | 1 | 1 | 2 | 0 | 0 | **2** | 0 | 0 | | | | | | | | | |
| MT | 2 | 2 | 2 | 2 | 2 | 2 | 0 | 0 | **2** | | | | | | | | |
| MSTd | 0 | 2 | 2 | 2 | 2 | 0 | 2 | 0 | 1 | **2** | | | | | | | |
| MSTl | 0 | 2 | 0 | 0 | 2 | 0 | 1 | 0 | 1 | **2** | **0** | | | | | | |
| FST | 0 | 1 | 2 | 1 | 2 | 2 | 1 | 0 | 2 | **2** | 2 | **2** | | | | | |
| PITd | 0 | 0 | 0 | 0 | 0 | **2** | 0 | **1** | **0** | **0** | 1 | 0 | **1** | | | | |
| PITv | 0 | 0 | 0 | 0 | 0 | 2 | 0 | **1** | 0 | 0 | 1 | 0 | 1 | **0** | | | |
| CITd | 0 | 0 | 0 | 0 | 0 | 2 | 0 | 0 | 0 | 0 | 0 | 0 | **0** | **0** | 1 | | |
| CITv | 0 | 0 | 0 | 0 | 0 | 2 | 0 | 0 | 0 | 0 | 0 | 0 | 0 | 1 | **2** | **0** | |
| PO | 2 | **1** | **1** | 1 | 1 | 0 | 2 | 0 | 1 | 1 | 2 | 2 | 0 | 0 | 0 | 0 | 0 |
| PIP | 2 | **1** | **2** | 2 | **0** | 2 | 2 | 0 | 0 | 2 | 0 | 0 | 0 | 0 | 0 | 0 | 0 |
| LIP | 0 | 0 | 2 | 1 | 1 | 2 | **2** | 0 | 0 | 2 | 2 | 1 | 2 | 0 | 1 | 0 | 0 |
| 7a | 0 | 0 | 0 | 0 | 0 | **0** | **2** | 0 | 0 | **0** | **2** | 0 | 1 | 0 | 0 | 0 | 0 |
| STPp | 0 | 0 | 0 | 0 | 0 | 0 | 0 | 0 | 0 | 0 | **2** | **2** | **2** | 0 | 0 | 1 | 1 |
| STPa | 0 | 0 | 0 | 0 | 0 | 0 | 0 | 0 | 0 | 0 | 0 | 0 | **0** | 0 | 0 | 0 | 0 |
| AITd | 0 | 0 | 0 | 0 | 0 | 0 | 0 | 0 | 0 | 0 | 0 | 0 | **0** | 1 | 1 | **1** | 2 |
| AITv | 0 | 0 | 0 | 0 | 0 | 2 | 0 | 0 | 0 | 0 | 0 | 0 | 0 | 1 | 2 | 1 | **2** |
| TF | 0 | **0** | 2 | **2** | 0 | **2** | 0 | **0** | 0 | 0 | 1 | 0 | 2 | 0 | **1** | 0 | **1** |
| TH | 0 | **0** | 0 | 0 | 0 | 2 | 0 | 0 | 0 | 0 | 0 | 0 | 0 | 0 | 1 | 1 | 1 |

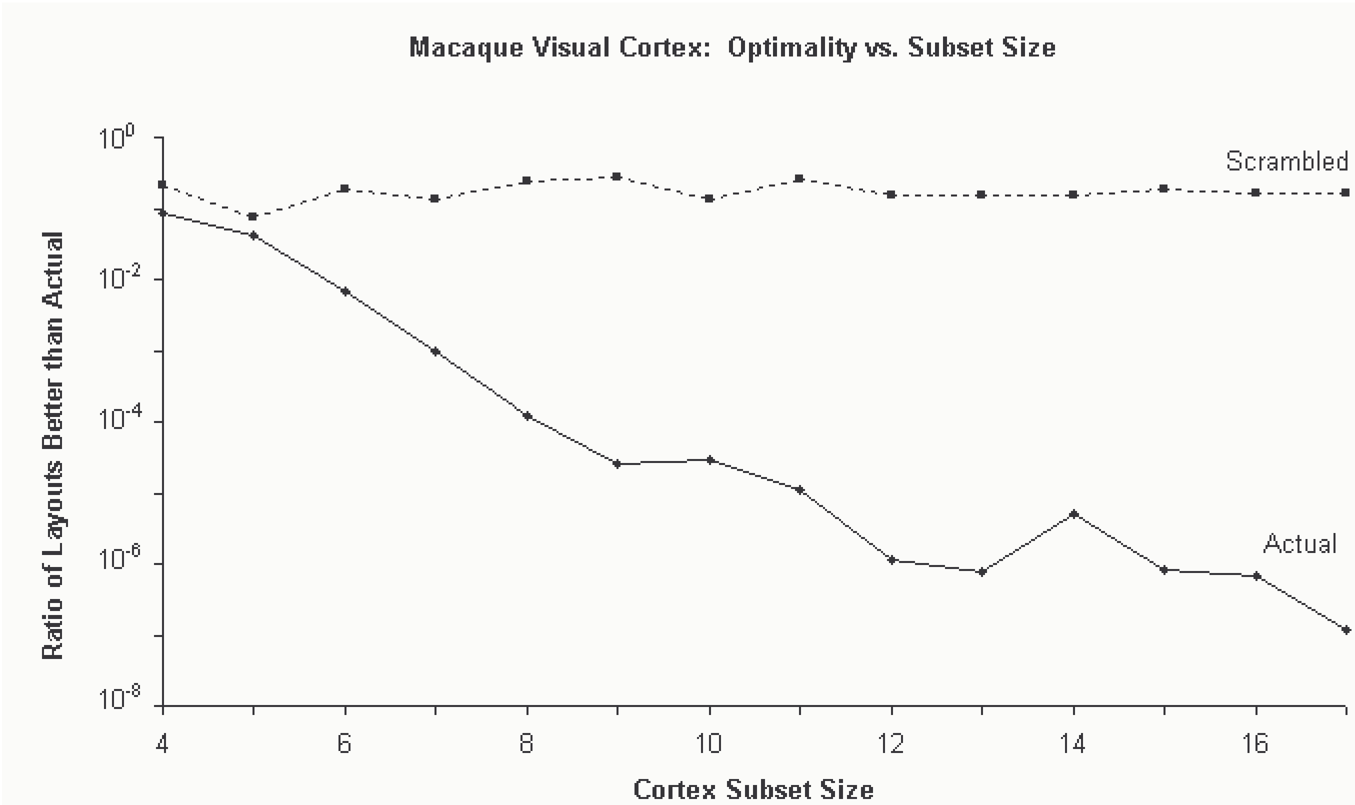


**Fig. S3**. Size Law for macaque visual cortex areas. The Size Law: If a set of connected components is optimally placed, then, the smaller a subset of that total layout, the less optimized it will tend to be. The system of components here is 17 contiguous macaque visual cortical areas as in Fig. S2, with connections and adjacencies as in Table S1. Optimality-measure is conformance of the system to the adjacency rule: If two components are connected, then they are adjacent to each other.(1) A layout is scored in terms of its number of violations of this "all or nothing" adjacency rule. A series of nested compact subsets of the set of cortical areas was generated, each consisting of from 4 to the full 17 areas. (Order of successive elements added is as in Table S1.) Each subset of the actual layout was compared with all possible alternative layouts of that subset for adjacency-rule optimality (16 and 17-element sets were each compared only with random samples of $10^9$ alternative layouts).

The "Actual layout" curve shows that smaller subsets rank approximately in the middle of their group of alternative layouts. But, as subset size increases, optimality-ranking of the actual layout consistently improves (with two exceptions, $p < 0.02$). Fewer than one in a million of all alternative layouts conform to the adjacency rule better than the actual layout of the complete 17-component set. For comparison, the "Scrambled layout" broken-line curve shows the corresponding analysis for a layout of the 17 visual areas with their adjacencies randomly shuffled; no Size Law trend toward improving optimality is now evident. Note that this analysis includes only 17 of the total 73 cortical areas.

Previous | Next

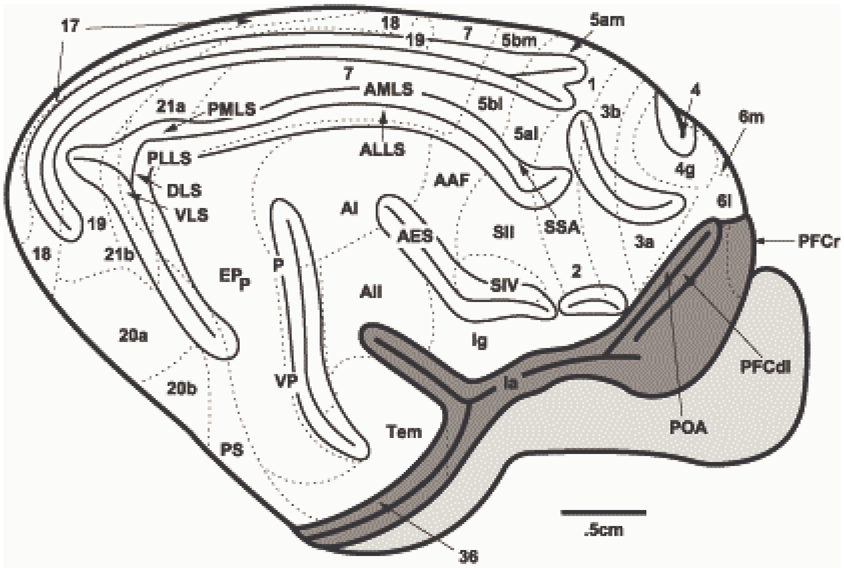


**Fig. S4** . Parcellation of cerebral cortex of cat. Placement of the interconnected functional areas is evaluated for how well total connection-costs are minimized. (A) Connection-cost optimization analysis of layout of 15 contiguous areas of the visual cortex, along with 13 immediately contiguous "edge" areas. 126 connections are reported among the core areas and with their edge areas. (B) Similar combined analysis of 39 areas of the visual, auditory, and somatosensory cortex, along with 14 edge-areas (451 connections reported). Core and edge areas are listed in Table S2 connection matrix below. Lateral aspect only is shown. Rostral is to right.(4)

**Table S2**. Combined connection and adjacency matrix for cat visual, auditory, and somatosensory cortex. The series of 39 core areas as in Fig. S4 is listed, in the order in which the areas are successively added to the analysis (17 - 6l). They are followed by the set of 14 edge areas for the total core (POA - Ig). A cell with 0 indicates no known connection between the area of that row and of that column; 1 - 6 indicates connection between the two areas. (Afferent and efferent connection weights of 1 - 3 have been summed.) Cell values in **bold** designate topological contiguity of the two areas on the cortex sheet, as in Fig. S4.(5)

| | | Visual | | | | | | | | | | | | | | | Auditory | | | | | | | | Somatosensory | | | | | | | | | | | | | | | | |
|---|---|---|---|---|---|---|---|---|---|---|---|---|---|---|---|---|---|---|---|---|---|---|---|---|---|---|---|---|---|---|---|---|---|---|---|---|---|---|---|---|---|
| | | 17 | 18 | 19 | 7 | AML | PML | 21a | 21b | ALLS | PLLS | VLS | DLS | 20a | 20b | PS | AI | AII | AAF | AES | P | VP | EPp | Tem | 5m | 5bm | 5bl | 5am | 5al | SSA | SII | SIV | 1 | 2 | 3b | 3a | 4 | 4q | 6m | 6l | |
| Visual | 18 | **6** | | | | | | | | | | | | | | | | | | | | | | | | | | | | | | | | | | | | | | | 18 |
| | 19 | 6 | **6** | | | | | | | | | | | | | | | | | | | | | | | | | | | | | | | | | | | | | | 19 |
| | 7 | **0** | **2** | **4** | | | | | | | | | | | | | | | | | | | | | | | | | | | | | | | | | | | | | 7 |
| | AMLS | 5 | 6 | 4 | **2** | | | | | | | | | | | | | | | | | | | | | | | | | | | | | | | | | | | | AMLS |
| | PMLS | 6 | 5 | 6 | **0** | **5** | | | | | | | | | | | | | | | | | | | | | | | | | | | | | | | | | | | PMLS |
| | 21a | 5 | 5 | **6** | **4** | 4 | **2** | | | | | | | | | | | | | | | | | | | | | | | | | | | | | | | | | | 21a |
| | 21b | 4 | 4 | **2** | 3 | 0 | 2 | **4** | | | | | | | | | | | | | | | | | | | | | | | | | | | | | | | | | 21b |
| | ALLS | 0 | 1 | 2 | 1 | **2** | 0 | 0 | 0 | | | | | | | | | | | | | | | | | | | | | | | | | | | | | | | | ALLS |
| | PLLS | 2 | 3 | 3 | 2 | 1 | **3** | 1 | 0 | **4** | | | | | | | | | | | | | | | | | | | | | | | | | | | | | | | PLLS |
| | VLS | 2 | 2 | 3 | 0 | 0 | **6** | 0 | **1** | 1 | **1** | | | | | | | | | | | | | | | | | | | | | | | | | | | | | | VLS |
| | DLS | 0 | 0 | 2 | 0 | 0 | 0 | 0 | 2 | 2 | **6** | **4** | | | | | | | | | | | | | | | | | | | | | | | | | | | | | DLS |
| | 20a | 6 | **4** | **6** | 3 | 0 | 6 | 4 | **4** | 0 | 3 | 4 | 0 | | | | | | | | | | | | | | | | | | | | | | | | | | | | 20a |
| | 20b | 0 | **0** | 2 | 2 | 2 | 0 | 0 | 0 | 0 | 0 | 0 | 0 | **6** | | | | | | | | | | | | | | | | | | | | | | | | | | | 20b |
| | PS | 0 | 0 | 1 | 1 | 1 | 1 | 1 | **1** | 0 | 6 | 0 | 0 | **2** | **4** | | | | | | | | | | | | | | | | | | | | | | | | | | PS |
| Auditory | AI | 0 | 0 | 0 | 0 | 0 | 0 | 0 | 0 | **0** | 0 | 0 | 0 | 0 | 0 | 0 | | | | | | | | | | | | | | | | | | | | | | | | | AI |
| | AII | 0 | 0 | 0 | 0 | 0 | 0 | 0 | 0 | 0 | 0 | 0 | 0 | 0 | 0 | 0 | **5** | | | | | | | | | | | | | | | | | | | | | | | | AII |
| | AAF | 0 | 0 | 0 | 0 | 0 | 0 | 0 | 0 | **0** | 0 | 0 | 0 | 0 | 0 | 0 | **6** | 4 | | | | | | | | | | | | | | | | | | | | | | | AAF |
| | AES | 0 | 0 | 0 | 0 | 2 | 2 | 1 | 0 | 4 | 6 | 1 | 4 | 2 | 3 | 4 | **0** | **1** | **1** | | | | | | | | | | | | | | | | | | | | | | AES |
| | P | 0 | 0 | 0 | 0 | 0 | 0 | 0 | 0 | 0 | 0 | 0 | 0 | 1 | 1 | 0 | **5** | **5** | 3 | 0 | | | | | | | | | | | | | | | | | | | | | P |
| | VP | 0 | 0 | 0 | 0 | 0 | 0 | 0 | 0 | 0 | 0 | 0 | 0 | 0 | 0 | 0 | 4 | **2** | 2 | 0 | **4** | | | | | | | | | | | | | | | | | | | | VP |
| | EPp | 0 | 0 | 1 | 3 | 0 | 0 | 2 | **2** | **1** | **1** | 1 | **2** | 4 | 4 | **2** | **2** | 3 | 1 | 2 | **4** | **4** | | | | | | | | | | | | | | | | | | | EPp |
| | Tem | 0 | 0 | 0 | 0 | 0 | 0 | 0 | 0 | 0 | 0 | 0 | 0 | 0 | 0 | **0** | 1 | **3** | 0 | 0 | 1 | **2** | **2** | | | | | | | | | | | | | | | | | | Tem |
| Somatosensory | 5m | 0 | 0 | 0 | **5** | 1 | 0 | 0 | 0 | 2 | 0 | 0 | 0 | 0 | 0 | 0 | 0 | 0 | 0 | 3 | 0 | 0 | 0 | 0 | | | | | | | | | | | | | | | | | 5m |
| | 5bm | 0 | 0 | 2 | **4** | 1 | 0 | 0 | 0 | 0 | 0 | 0 | 0 | 0 | 0 | 0 | 0 | 0 | 0 | 3 | 0 | 0 | 0 | 0 | **4** | | | | | | | | | | | | | | | | 5bm |
| | 5bl | 0 | 1 | 3 | **5** | **2** | 2 | 2 | 2 | 2 | 1 | 0 | 0 | 0 | 0 | 0 | 0 | 0 | **0** | 0 | 0 | 0 | 0 | 0 | 2 | **4** | | | | | | | | | | | | | | | 5bl |
| | 5am | 0 | 0 | 0 | 2 | 1 | 0 | 0 | 0 | 0 | 0 | 0 | 0 | 0 | 0 | 0 | 0 | 0 | 0 | 3 | 0 | 0 | 0 | 0 | **4** | **6** | 0 | | | | | | | | | | | | | | 5am |
| | 5al | 0 | 0 | 2 | 4 | 2 | 0 | 1 | 1 | 0 | 0 | 0 | 0 | 2 | 2 | 0 | 0 | 0 | 0 | 3 | 0 | 0 | 0 | 0 | 4 | 3 | **5** | **3** | | | | | | | | | | | | | 5al |
| | SSA | 0 | 0 | 0 | 4 | 0 | 0 | 0 | 0 | 0 | 0 | 0 | 0 | 0 | 0 | 0 | 0 | 0 | 0 | 3 | 0 | 0 | 0 | 0 | 3 | 3 | **4** | 5 | **5** | | | | | | | | | | | | SSA |
| | SII | 0 | 0 | 0 | 0 | 0 | 0 | 0 | 0 | 0 | 0 | 0 | 0 | 0 | 0 | 0 | 0 | 0 | **0** | 2 | 0 | 0 | 0 | 0 | 2 | 4 | 2 | 3 | 2 | **0** | | | | | | | | | | | SII |
| | SIV | 0 | 0 | 0 | 0 | 0 | 0 | 0 | 0 | 0 | 0 | 0 | 0 | 0 | 0 | 0 | 0 | 0 | **0** | **4** | 0 | 0 | 0 | 0 | 3 | 4 | 0 | 4 | 4 | 2 | **1** | | | | | | | | | | SIV |
| | 1 | 0 | 0 | 0 | 0 | 0 | 0 | 0 | 0 | 0 | 0 | 0 | 0 | 0 | 0 | 0 | 0 | 0 | 0 | 0 | 0 | 0 | 0 | 0 | **2** | 2 | 1 | **3** | **1** | **1** | 6 | 0 | | | | | | | | | 1 |
| | 2 | 0 | 0 | 0 | 0 | 0 | 0 | 0 | 0 | 0 | 0 | 0 | 0 | 0 | 0 | 0 | 0 | 0 | 0 | 0 | 0 | 0 | 0 | 0 | 2 | 0 | 0 | 2 | 2 | **2** | **6** | **0** | **4** | | | | | | | | 2 |
| | 3b | 0 | 0 | 0 | 0 | 0 | 0 | 0 | 0 | 0 | 0 | 0 | 0 | 0 | 0 | 0 | 0 | 0 | 0 | 2 | 0 | 0 | 0 | 0 | **1** | 1 | 0 | 2 | 3 | 2 | 6 | 1 | **4** | **4** | | | | | | | 3b |
| | 3a | 0 | 0 | 0 | 0 | 0 | 0 | 0 | 0 | 0 | 0 | 0 | 0 | 0 | 0 | 0 | 0 | 0 | 0 | 2 | 0 | 0 | 0 | 0 | 0 | 0 | 0 | 3 | 3 | 1 | 6 | 0 | 4 | 4 | **4** | | | | | | 3a |
| | 4 | 0 | 0 | 0 | 0 | 1 | 0 | 0 | 0 | 0 | 0 | 0 | 0 | 0 | 0 | 0 | 0 | 0 | 0 | 2 | 0 | 0 | 0 | 0 | 4 | 4 | 3 | 4 | 2 | 2 | 5 | 1 | 3 | 3 | 4 | **4** | | | | | 4 |
| | 4g | 0 | 0 | 0 | 1 | 1 | 0 | 0 | 0 | 0 | 0 | 0 | 0 | 0 | 0 | 0 | 0 | 0 | 0 | 3 | 0 | 0 | 0 | 0 | 4 | 5 | 2 | 5 | 5 | 4 | 5 | 1 | 4 | 4 | 4 | **5** | **4** | | | | 4g |
| | 6m | 0 | 0 | 0 | 6 | 1 | 0 | 0 | 0 | 1 | 1 | 0 | 0 | 1 | 1 | 0 | 0 | 0 | 0 | 3 | 0 | 0 | 3 | 0 | 2 | 2 | 4 | 2 | 2 | 4 | 1 | 4 | 1 | 1 | 0 | 0 | **0** | **3** | | | 6m |
| | 6l | 0 | 0 | 1 | 4 | 0 | 1 | 0 | 0 | 0 | 1 | 0 | 0 | 1 | 1 | 0 | 0 | 0 | 0 | 1 | 0 | 0 | 1 | 0 | 2 | 2 | 3 | 0 | 4 | 2 | 2 | 4 | 2 | 2 | 2 | **2** | 2 | **2** | **6** | | 6l |
| Edge | POA | 0 | 0 | 0 | 2 | 0 | 0 | 0 | 0 | 0 | 0 | 0 | 0 | 1 | 1 | 0 | 0 | 0 | 0 | 4 | 0 | 0 | 0 | 0 | 0 | 0 | 2 | 0 | 0 | 0 | 3 | 4 | 0 | 0 | **1** | **1** | 0 | 0 | 2 | **0** | POA |
| | 36 | 0 | 0 | 0 | 0 | 1 | 1 | 1 | 1 | 1 | 1 | 0 | 0 | 2 | 2 | **4** | 1 | 3 | 2 | 3 | 0 | 1 | 3 | **6** | 0 | 1 | 0 | 0 | 0 | 0 | 2 | 3 | 1 | 1 | 1 | 1 | 1 | 0 | 2 | 0 | 36 |
| | ER | 0 | 0 | 0 | 0 | 0 | 0 | 0 | 0 | 0 | 0 | 0 | 0 | 2 | **2** | 0 | 0 | 0 | 0 | 0 | 0 | 0 | 0 | 0 | 0 | 0 | 0 | 0 | 0 | 0 | 0 | 0 | 0 | 0 | 0 | 0 | 1 | 0 | 2 | 0 | ER |
| | PSb | 0 | 0 | 0 | 0 | 0 | 0 | 0 | 0 | 0 | 0 | 0 | 0 | 1 | **1** | 0 | 0 | 0 | 0 | 0 | 0 | 0 | 0 | 0 | 0 | 0 | 0 | 0 | 0 | 0 | 0 | 0 | 0 | 0 | 0 | 0 | 0 | 0 | 0 | 0 | PSb |
| | RS | 0 | 0 | 0 | 2 | 0 | 0 | 0 | 0 | 0 | 0 | 0 | 0 | 4 | **4** | 0 | 0 | 0 | 0 | 0 | 4 | 0 | 0 | 0 | 0 | 0 | 0 | 0 | 0 | 0 | 0 | 0 | 0 | 0 | 0 | 0 | 0 | 0 | 0 | 0 | RS |
| | CGp | **0** | 0 | 0 | 6 | 0 | 0 | 0 | 0 | 0 | 0 | 0 | 0 | 3 | 3 | 0 | 0 | 0 | 0 | 3 | 4 | 1 | 4 | 0 | 0 | 0 | 0 | 0 | 0 | 0 | 0 | 0 | 0 | 0 | 0 | 0 | 0 | 0 | 6 | 0 | CGp |
| | CGa | **0** | 0 | 0 | **1** | 1 | 1 | 0 | 0 | 1 | 1 | 1 | 1 | 2 | 3 | 1 | 0 | 0 | 0 | 3 | 4 | 0 | 2 | 0 | **2** | 3 | 2 | 2 | 2 | 3 | 0 | 1 | 0 | 0 | **0** | **0** | **2** | 2 | **5** | 3 | CGa |
| | LA | 0 | 0 | 0 | 1 | 1 | 0 | 0 | 0 | 0 | 0 | 0 | 0 | 0 | 1 | 1 | 0 | 0 | 0 | 0 | 0 | 0 | 1 | 0 | 2 | 3 | 2 | 2 | 2 | 3 | 0 | 1 | 0 | 0 | 0 | 0 | 2 | 2 | **2** | 2 | LA |
| | PL | 0 | 0 | 0 | 0 | 0 | 0 | 0 | 0 | 0 | 0 | 0 | 0 | 0 | 0 | 0 | 0 | 0 | 0 | 0 | 0 | 0 | 0 | 2 | 0 | 0 | 0 | 0 | 0 | 0 | 0 | 0 | 0 | 0 | 0 | 0 | 0 | 0 | **4** | 2 | PL |
| | PFCdm | 0 | 0 | 0 | 2 | 0 | 0 | 0 | 0 | 1 | 1 | 0 | 0 | 0 | 0 | 2 | 0 | 1 | 0 | 0 | 0 | 0 | 2 | 0 | 0 | 0 | 0 | 0 | 0 | 0 | 0 | 1 | 0 | 0 | 0 | 0 | 0 | 0 | **2** | **1** | PFCdm |
| | PFCr | 0 | 0 | 0 | 2 | 0 | 0 | 0 | 0 | 0 | 0 | 0 | 0 | 0 | 0 | 0 | 0 | 1 | 0 | 2 | 0 | 0 | 0 | 1 | 0 | 0 | 0 | 0 | 0 | 0 | 0 | 0 | 0 | 0 | 0 | 0 | 0 | 0 | 1 | **1** | PFCr |
| | PFCdl | 0 | 0 | 0 | 2 | 0 | 0 | 0 | 0 | 1 | 1 | 0 | 0 | 2 | 2 | 2 | 0 | 1 | 0 | 3 | 0 | 0 | 2 | 1 | 0 | 0 | 2 | 0 | 2 | 0 | 0 | 1 | 0 | 0 | 0 | 0 | 0 | 0 | 2 | **2** | PFCdl |
| | Ia | 0 | 0 | 0 | 1 | 0 | 1 | 0 | 0 | 1 | 2 | 0 | 2 | 2 | 1 | 1 | 1 | **3** | 0 | 2 | 0 | 0 | 4 | **2** | 2 | 2 | 2 | 2 | 3 | 2 | 2 | 3 | 0 | 1 | 0 | 0 | 0 | 0 | 4 | 0 | Ia |
| | Ig | 0 | 0 | 0 | 2 | 0 | 1 | 0 | 0 | 3 | 3 | 0 | 2 | 2 | 1 | 5 | 1 | **3** | 0 | **4** | 0 | 0 | 4 | 2 | 1 | 1 | 1 | 1 | 2 | 1 | **2** | **4** | 0 | **1** | 0 | 0 | 1 | 1 | 4 | 1 | Ig |
| | | 17 | 18 | 19 | 7 | AML | PML | 21a | 21b | ALLS | PLLS | VLS | DLS | 20a | 20b | PS | AI | AII | AAF | AES | P | VP | EPp | Tem | 5m | 5bm | 5bl | 5am | 5al | SSA | SII | SIV | 1 | 2 | 3b | 3a | 4 | 4q | 6m | 6l | |

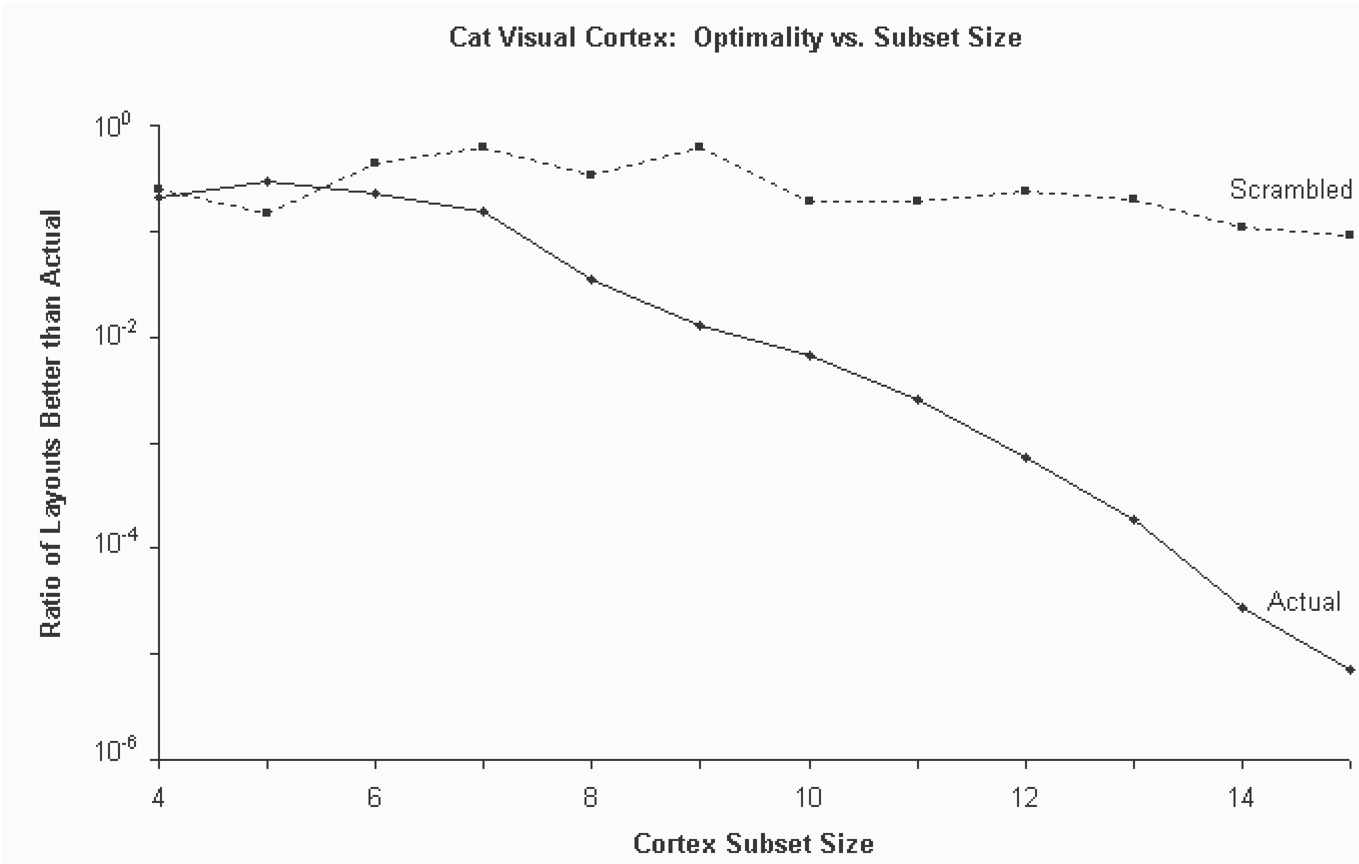


**Fig. S5**. Size Law for cat visual cortex areas. The system of components here is the 15 contiguous cat visual cortical areas in Fig. S4 (17 - PS), with connections and adjacencies as in Table S2. Optimality-measure is conformance of the system to the "all or nothing" adjacency rule, with each layout scored in terms of its number of violations of the rule. A series of nested compact subsets of the set of cortex areas was generated, each consisting of from 4 to the full 15 areas. Each subset of the actual layout was compared with all possible alternative layouts of that subset for adjacency-rule optimality.

The "Actual layout" curve shows that smaller subsets rank approximately in the middle of their group of alternative layouts. But, again, as subset size increases, optimality-ranking of the actual layout consistently improves (with one exception, $\underline{p} < 0.02$). Only one in a hundred thousand of all alternative layouts conform to the adjacency rule better than the actual layout of the complete 15-component set. For comparison, the "Scrambled layout" broken-line curve shows the corresponding analysis for a layout of the 15 visual areas with their adjacencies randomly shuffled; no Size Law trend toward improving optimality is evident. Note that this analysis includes only 15 of the total 57 cortical areas.

Previous | Next

**Table S3** . Combined connection and adjacency matrix for "metamodules" composed from areas of cat visual, auditory, and somatosensory cortex. The series of 14 metamodules, each constructed from the areas in Fig. S4 above, with connections and adjacencies from Table S2, is listed in the order in which the areas are successively added to the analysis. They are followed by the set of 13 edge areas for the total core. A cell with 0 indicates no known connection between the metamodule of that row and of that column; 1 - 44 indicates connection between the two metamodules. (Afferent and efferent connection weights of all areas in the two metamodules have been summed. A total 134 connections are included. Cell values in **bold** designate topological contiguity of the two metamodules on the cortex sheet, as in Fig. S4.

| | V1 | V2 | V3 | V4 | V5 | A1 | A2 | A3 | S1 | S2 | S3 | S4 | S5 | S6 |
|---|---|---|---|---|---|---|---|---|---|---|---|---|---|---|
| V2 | **12** | | | | | | | | | | | | | |
| V3 | **9** | **23** | | | | | | | | | | | | |
| V4 | 6 | **13** | **16** | | | | | | | | | | | |
| V5 | 15 | 37 | **17** | 23 | | | | | | | | | | |
| A1 | 0 | 0 | 0 | 0 | **0** | | | | | | | | | |
| A2 | 0 | 0 | 1 | 11 | 19 | **24** | | | | | | | | |
| A3 | 0 | 1 | **7** | **10** | **5** | **4** | **19** | | | | | | | |
| S1 | 0 | 8 | **30** | 4 | **14** | **0** | 15 | 0 | | | | | | |
| S2 | 0 | 0 | 0 | 0 | 0 | **0** | **6** | 0 | **30** | | | | | |
| S3 | 0 | 0 | 0 | 0 | 0 | 0 | 0 | 0 | **18** | **12** | | | | |
| S4 | 0 | 0 | 0 | 0 | 0 | 0 | 4 | 0 | **16** | 13 | **16** | | | |
| S5 | 0 | 0 | 1 | 0 | 2 | 0 | 5 | 0 | 44 | 12 | 14 | **17** | | |
| S6 | 0 | 1 | 12 | 6 | 5 | 0 | 8 | 4 | 31 | 18 | 6 | **6** | **7** | |
| 36 | 0 | 0 | 2 | **8** | 4 | 3 | 7 | **9** | 1 | 5 | 2 | 2 | 1 | 2 |
| ER | 0 | 0 | 0 | **4** | 0 | 0 | 0 | 0 | 0 | 0 | 0 | 0 | 1 | 2 |
| PSb | 0 | 0 | 0 | **2** | 0 | 0 | 0 | 0 | 0 | 0 | 0 | 0 | 0 | 0 |
| RS | 0 | 0 | 2 | **8** | 0 | 0 | 4 | 0 | 0 | 0 | 0 | 0 | 0 | 0 |
| CGp | **0** | 0 | 6 | 6 | 0 | 0 | 8 | 4 | 0 | 0 | 0 | 0 | 0 | 10 |
| CGa | **0** | 0 | **1** | 6 | 6 | 0 | 7 | 2 | **14** | 1 | 0 | **0** | **4** | **8** |
| LA | 0 | 0 | 1 | 2 | 1 | 0 | 0 | 1 | 14 | 1 | 0 | 0 | 4 | **4** |
| PL | 0 | 0 | 0 | 0 | 0 | 0 | 0 | 2 | 0 | 0 | 0 | 0 | 0 | **6** |
| PFCdm | 0 | 0 | 2 | 2 | 2 | 0 | 1 | 2 | 0 | 1 | 0 | 0 | 0 | **3** |
| PFCr | 0 | 0 | 2 | 0 | 0 | 0 | 3 | 1 | 0 | 0 | 0 | 0 | 0 | **2** |
| PFCdl | 0 | 0 | 2 | 6 | 2 | 0 | 4 | 3 | 4 | 1 | 0 | 0 | 0 | **4** |
| Ia | 0 | 0 | 1 | 4 | 6 | 1 | **5** | **6** | 13 | 5 | 1 | 0 | 0 | **5** |
| Ig | 0 | 0 | 2 | 8 | 9 | 1 | **7** | 6 | 7 | **6** | **1** | 0 | 2 | **7** |

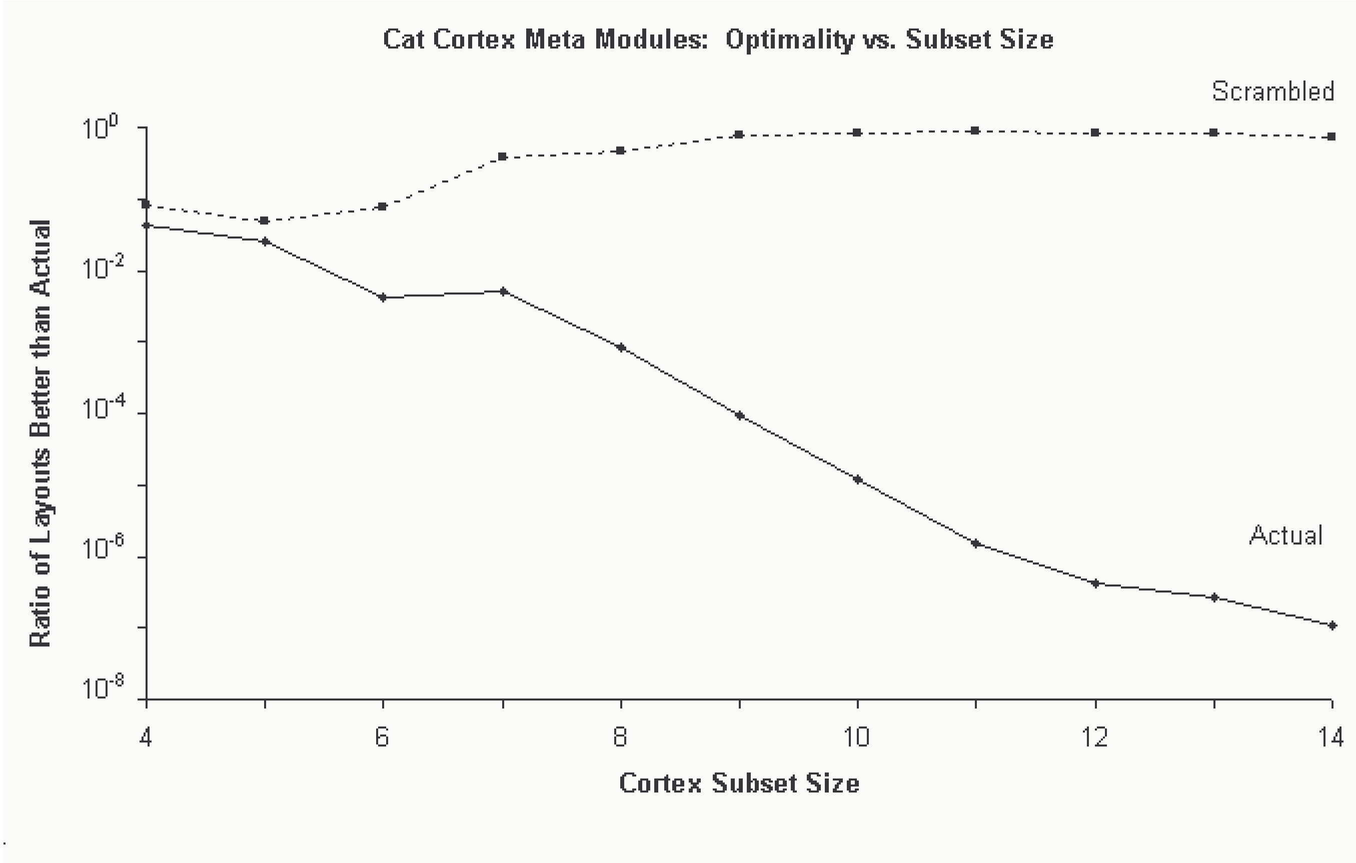


**Fig. S6**. Size Law for cat cortex "metamodules". If a set of connected components is optimally placed, then a set of metamodules each consisting of a subset of those components in the same positions will also be optimally placed. 40 Brodmann areas of the visual, auditory, and somatosensory regions of the cat cortex are grouped into 14 such modules, with connections and adjacencies as in Table S3. A series of nested subsets of those metamodules was then generated. The same Size Law trend of optimality improvement of the actual metamodule layout with increasing subset size is evident as for the actual layout of individual areas of the cat visual cortex: As subset size increases, optimality-ranking of actual layout consistently improves (with one exception, $p < 0.02$). (Exhaustive searches of all alternative layouts were performed.)

However, since 40 individual areas are now incorporated in these 14 metamodules, the Size Law furthermore implies that such a larger subset of the total 57-area cortical system should show better optimization than the 15-area visual subset. Such improvement is evident here: For example, by a subset size of 11 metamodules (consisting of 31 cortical areas), the actual layout's top $\sim 10^{-6}$ rank exceeds the full 15-area visual system's rank; the full 14-metamodule actual layout ranks in the top $1.09 \times 10^{-7}$ of all 14! possible alternative layouts--almost 100 times better than the full 15-area visual system. "Scrambled layout" broken-line curve shows corresponding analysis for a randomly shuffled layout of the meta-modules; no Size Law trend is evident.

Previous | Next

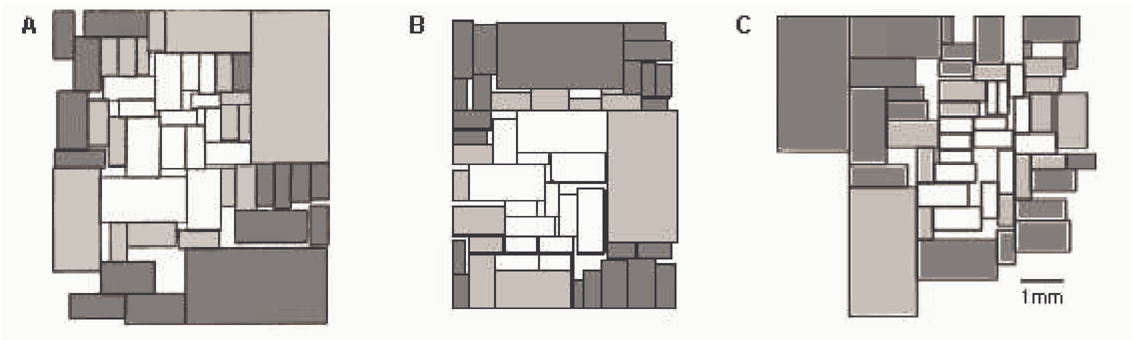


**Fig. S7** . Integrated circuit networks for calibration of optimality analysis: AMI49 microchip, the largest of the MCNC set of benchmark circuits, with 49 modules.(6) (**A**) Esbensen and Kuh layout; cost to be minimized is a function of layout area and maximum path delay.(7) (**B**) Hong et al layout; cost to be minimized is a function of area and total wirelength.(8) (**C**) Lin and Chang layout; cost to be minimized is total wirelength.(9) In each case, the central 15 blocks (white), along with the surrounding edge-zone of immediately contiguous blocks (light gray), was analyzed. Again, placement of the interconnected areas is evaluated for how well total interconnection costs--adjacency rule violations--are minimized. Core and edge areas for Lin and Chang layout are listed in Table S4 connection matrix below.

**Table S4**. Combined connection and adjacency matrix for Lin and Chang layout of AMI49 microchip. The series of 15 core blocks shown above in Fig. S7C is listed (M014 - M020), in the order in which the areas are successively added to the analysis. They are followed by the set of 14 edge blocks for the total core (M030 - M032). (There are 103 connections among the core blocks and with the edge blocks.) A cell with 0 indicates no connection between the area of that row and of that column; 1 - 14 indicates connection density between the two areas. Cell values in **bold** designate topological contiguity of the two areas on the chip, as in Fig. S7C.

| | 1 | 2 | 3 | 4 | 5 | 6 | 7 | 8 | 9 | 10 | 11 | 12 | 13 | 14 | 15 |
|---|---|---|---|---|---|---|---|---|---|---|---|---|---|---|---|
| | M014 | M025 | M021 | M017 | M016 | M036 | M037 | M034 | M035 | M031 | M029 | M041 | M039 | M024 | M020 |
| M025 | **4** | | | | | | | | | | | | | | |
| M021 | **1** | **4** | | | | | | | | | | | | | |
| M017 | 0 | 0 | **0** | | | | | | | | | | | | |
| M016 | 0 | 2 | 0 | **10** | | | | | | | | | | | |
| M036 | 4 | 5 | 1 | 0 | **0** | | | | | | | | | | |
| M037 | 0 | 0 | 0 | 0 | 0 | **0** | | | | | | | | | |
| M034 | 0 | 2 | 0 | 0 | 0 | 6 | **0** | | | | | | | | |
| M035 | 0 | 0 | 0 | 0 | 0 | 2 | 0 | **8** | | | | | | | |
| M031 | 0 | 1 | 1 | 0 | 0 | 3 | 0 | 3 | **2** | | | | | | |
| M029 | 0 | 2 | 1 | 0 | 0 | 1 | 0 | 0 | 0 | **1** | | | | | |
| M041 | 0 | 0 | 0 | 0 | 0 | 0 | 0 | 0 | 0 | 0 | **0** | | | | |
| M039 | 0 | 0 | 0 | 0 | 0 | 0 | 13 | 0 | 0 | 0 | 0 | **0** | | | |
| M024 | 0 | 1 | 1 | 0 | 0 | 2 | 0 | 0 | 0 | 1 | 1 | 0 | **0** | | |
| M020 | 0 | 0 | 2 | 0 | 0 | 0 | 0 | 0 | 0 | 0 | 0 | 0 | 0 | **0** | |
| M030 | 2 | 0 | 0 | 0 | 2 | 2 | 0 | 4 | 2 | 14 | **0** | 0 | 0 | 2 | 0 |
| M004 | 0 | 1 | 1 | 0 | 0 | 0 | **0** | 1 | 0 | 0 | 0 | 0 | 0 | 0 | 0 |
| M049 | 0 | 0 | 0 | 0 | 0 | 1 | 0 | 0 | **0** | **0** | 0 | 0 | 0 | 0 | 0 |
| M018 | 1 | 2 | 2 | 9 | 0 | 1 | 0 | 0 | 0 | **1** | **1** | 0 | 0 | 1 | 0 |
| M027 | 0 | 3 | 0 | 0 | 0 | 2 | 0 | 1 | 0 | 0 | **4** | 2 | 0 | 0 | 0 |
| M046 | 0 | 1 | 0 | 0 | 0 | 0 | 0 | 0 | 0 | 0 | 0 | 1 | 0 | 0 | 0 |
| M043 | 0 | 0 | 0 | 0 | 0 | 0 | 0 | 1 | 0 | 0 | 0 | **7** | 0 | 0 | 0 |
| M040 | 0 | 2 | 1 | 0 | 0 | 1 | 0 | 0 | 0 | 1 | 2 | 0 | **0** | 1 | 0 |
| M038 | 0 | 2 | 1 | 0 | 0 | 1 | 5 | 0 | 0 | 1 | 1 | 0 | **12** | 1 | 0 |
| M019 | 1 | 5 | 6 | 1 | 0 | 2 | 1 | 1 | 0 | 1 | 1 | 0 | **0** | **3** | **2** |
| M023 | 0 | 0 | 4 | 0 | 0 | 0 | 0 | 0 | 0 | 0 | 0 | 0 | 0 | 6 | **0** |
| M022 | 0 | **2** | **1** | 0 | 0 | 0 | 0 | 0 | 0 | 0 | 0 | 0 | 0 | 0 | 0 |
| M008 | 0 | 1 | **1** | **0** | 0 | 2 | 0 | 0 | 0 | 1 | 1 | 0 | 0 | 1 | 0 |
| M015 | 1 | 1 | 1 | 0 | 2 | **1** | **0** | 0 | 0 | 0 | 0 | 1 | 0 | 0 | 0 |
| M032 | 4 | 4 | 2 | 0 | 0 | 9 | **0** | **5** | 0 | 1 | 1 | 0 | 0 | 2 | 0 |

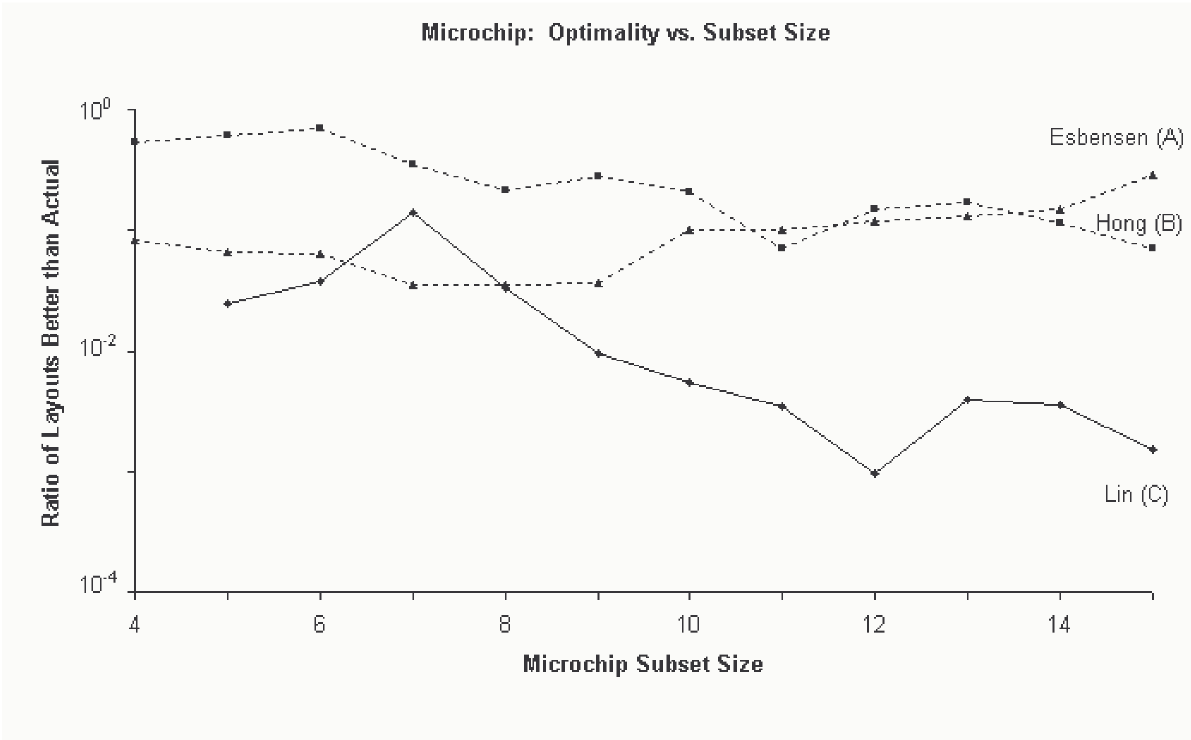


**Fig. S8**. Size Law for three layouts of AMI49 chip. In each case, the system of components is 15 contiguous central blocks as in Fig. S7; connections and adjacencies for Lin and Chang are as in Table S4. Optimality-measure is conformance of the system to the adjacency rule, with a layout scored in terms of number of violations of the "all or nothing" adjacency rule. A series of nested compact subsets of the set of blocks was generated, each consisting of from 4 to the full 15 areas. (For the Lin and Chang layout, order of successive elements added is as in Table S4.) Each subset of the actual layout was compared with all possible alternative layouts of that subset for adjacency-rule optimality (14 and 15-element sets were each compared only with random samples of $10^9$ alternative layouts).

The curve for the Lin and Chang layout (**C**) shows the same Size Law pattern as the cortex networks earlier, although somewhat weaker; the full 15-component subset only attains an optimality-rank of $1.5 \times 10^{-3}$. Both Esbensen and Kuh (**A**), and Hong et al (**B**), layouts do not show a Size Law pattern, nor does either attain significant optimality. So, for these calibration networks, adjacency rule conformance seems capable of distinguishing wirelength minimization from some other related cost-measures. Note that the analysis includes only 15 of the total system of 49 modules. (See also Fig. S1 above.)

Previous | Next

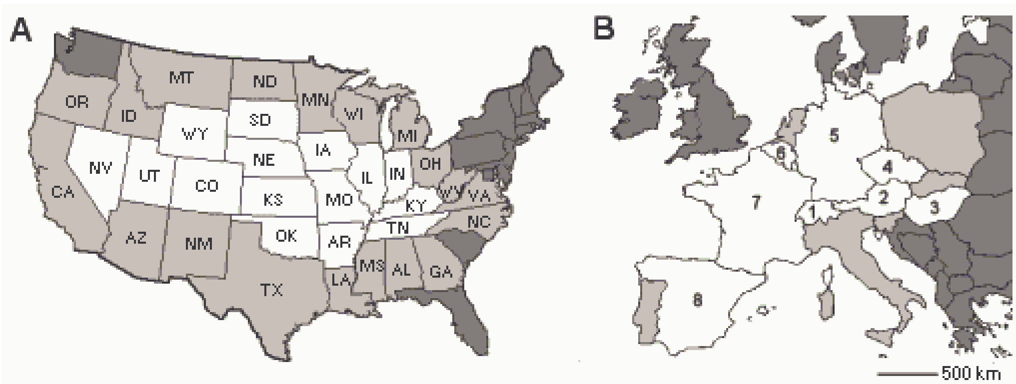


**Fig. S9.** Macroeconomic commodity-flow networks. (A) U.S. interstate commodity flow.(10) The central 15 states (white), along with the surrounding edge-zone of 19 immediately contiguous states (light gray), were analyzed. Core and edge areas for USA15 states are listed in Table S5 connection matrix below. (B) European international commodity flow.(11) The central 8 countries (white), along with a fragmentary surrounding edge-zone of 6 immediately contiguous countries (light gray), were analyzed as pilot data.

**Table S5**. Combined "connection" and adjacency matrix for U.S. interstate commodity flow (1997 Survey Sample). The series of 15 core states shown above in Fig. S9A is listed (KS - OK), in the order in which the areas are successively added to the analysis. They are followed by the set of 19 edge states for the total core (TX - LA). Cell values are in $ millions. An all-or-nothing cutoff threshold was set to yield approximately the same connectivity density as macaque and cat cortex above (see Table S7): If "export" + "import" flow between two states exceeds $ 1,500,000,000, a connection is recorded; sub-threshold economic transactions between the state of a row and the state of a column count as no connection. Cell values in bold designate topological contiguity of the two states, as in Fig. S9A.

| | KS | CO | UT | NV | WY | SD | NE | IA | MO | IL | IN | KY | TN | AR | OK |
|---|---|---|---|---|---|---|---|---|---|---|---|---|---|---|---|
| CO | **2885** | | | | | | | | | | | | | | |
| UT | 755 | **2976** | | | | | | | | | | | | | |
| NV | 26 | 824 | **3507** | | | | | | | | | | | | |
| WY | 258 | **2113** | **826** | 137 | | | | | | | | | | | |
| SD | 344 | 653 | 401 | 0 | **146** | | | | | | | | | | |
| NE | **4384** | **2623** | 410 | 0 | **449** | **1373** | | | | | | | | | |
| IA | 3242 | 1582 | 536 | 255 | 224 | **2029** | **7700** | | | | | | | | |
| MO | **15773** | 2987 | 1605 | 360 | 453 | 144 | **3225** | **6793** | | | | | | | |
| IL | 5971 | 4794 | 1010 | 893 | 551 | 842 | 4964 | **17277** | **24981** | | | | | | |
| IN | 2234 | 1715 | 892 | 429 | 269 | 598 | 1659 | 4900 | 10785 | **36898** | | | | | |
| KY | 1175 | 1152 | 798 | 319 | 6 | 58 | 457 | 1656 | **3700** | **9578** | **13761** | | | | |
| TN | 2011 | 1585 | 799 | 548 | 71 | 250 | 775 | 2377 | **5735** | 10844 | 8345 | **12690** | | | |
| AR | 1590 | 628 | 362 | 250 | 181 | 36 | 570 | 1511 | **7237** | 4562 | 2993 | 2191 | **6246** | | |
| OK | **3896** | **1382** | 516 | 237 | 364 | 51 | 815 | 1598 | **3850** | 3231 | 1343 | 869 | 1854 | **3685** | |
| TX | 9197 | 8826 | 3136 | 1608 | 556 | 933 | 4920 | 6021 | 13838 | 26051 | 14220 | 9133 | 13514 | **12630** | **20480** |
| NM | 219 | **1512** | 464 | 193 | 45 | 0 | 240 | 141 | 465 | 610 | 440 | 313 | 246 | 183 | **402** |
| AZ | 1198 | 2029 | **2075** | **2457** | 84 | 0 | 418 | 874 | 2317 | 2321 | 1730 | 700 | 2079 | 1053 | 577 |
| CA | 8542 | 15459 | 10888 | **20494** | 470 | 1797 | 5191 | 6160 | 15928 | 29183 | 10677 | 11997 | 12958 | 6649 | 7849 |
| OR | 633 | 1748 | 1192 | **824** | 438 | 199 | 495 | 926 | 1197 | 3138 | 2485 | 1188 | 1099 | 513 | 559 |
| ID | 345 | 1191 | **2732** | **676** | **258** | 48 | 310 | 303 | 363 | 949 | 316 | 60 | 322 | 103 | 32 |
| MT | 235 | 804 | 678 | 152 | **630** | **343** | 248 | 477 | 91 | 772 | 304 | 123 | 198 | 166 | 351 |
| ND | 2635 | 2778 | 1885 | 682 | 223 | **191** | 2887 | 4828 | 13442 | 30441 | 30737 | 12361 | 9542 | 2062 | 3004 |
| MN | 256 | 67 | 32 | 3 | 47 | **848** | 325 | **1134** | 403 | 1308 | 524 | 0 | 304 | 179 | 205 |
| WI | 2104 | 1834 | 1005 | 304 | 259 | 3862 | 3160 | **9345** | 3957 | **16164** | 4928 | 2293 | 3003 | 1319 | 1446 |
| MI | 2485 | 2905 | 1098 | 733 | 303 | 1570 | 1901 | 6815 | 4898 | 32094 | **7644** | 3271 | 5070 | 1628 | 1795 |
| OH | 4279 | 3082 | 2076 | 1148 | 192 | 668 | 2334 | 6774 | 9986 | 32937 | **33056** | **20618** | 7652 | 3691 | 1754 |
| WV | 163 | 34 | 70 | 18 | 19 | 7 | 78 | 133 | 699 | 1732 | 1161 | **2950** | 1277 | 158 | 88 |
| VA | 779 | 1758 | 608 | 256 | 63 | 163 | 809 | 1485 | 2289 | 6499 | 3385 | **5273** | **7368** | 1164 | 1597 |
| NC | 2216 | 1578 | 375 | 545 | 86 | 126 | 1020 | 2392 | 5148 | 9085 | 5549 | 5883 | **10623** | 2096 | 1622 |
| GA | 1929 | 1883 | 1189 | 568 | 139 | 97 | 1242 | 2506 | 7432 | 11852 | 7164 | 6451 | **19411** | 3620 | 1558 |
| AL | 965 | 393 | 218 | 18 | 39 | 66 | 269 | 934 | 2528 | 4853 | 3976 | 3138 | **10948** | 2096 | 995 |
| MS | 652 | 380 | 261 | 88 | 5 | 204 | 579 | 706 | 1941 | 3209 | 2035 | 1668 | **7364** | **4227** | 816 |
| LA | 1161 | 576 | 167 | 145 | 154 | 4 | 436 | 2660 | 3046 | 9494 | 3352 | 3628 | 4813 | **4880** | 1876 |

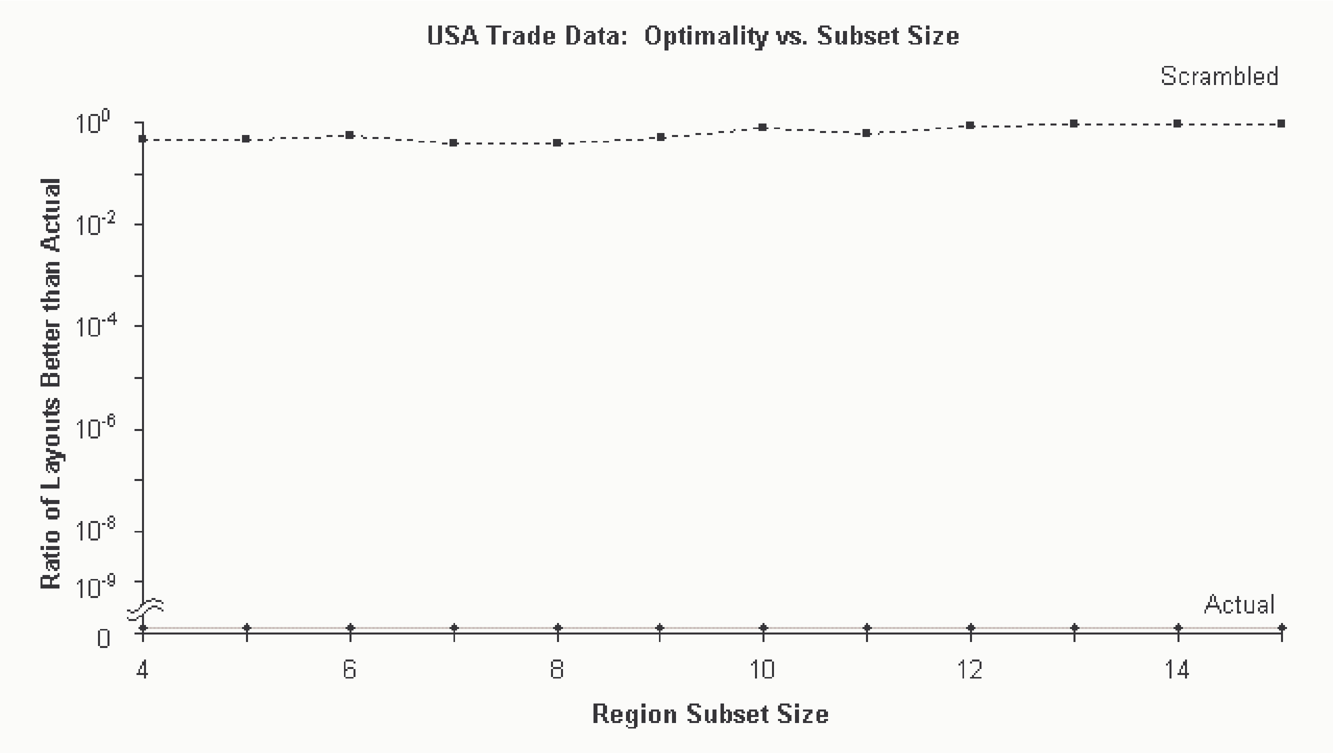


**Fig. S10**. Size Law performance for commodity flow among 15 U.S. states (BTS). The system of components here is a core of contiguous economic zones as in Fig. S9, with "connections" and adjacencies as in Table S5. For evaluation of how well total interconnection costs are minimized, optimality-measure is conformance of the system to the "all or nothing" adjacency rule: each layout is scored in terms of its number of violations of the rule. A series of nested compact subsets of the set of zones was generated (order of successive states added is as in Table S5). Each subset of the actual layout was compared with all possible alternative layouts of that subset for adjacency-rule optimality (14 and 15-element sets were each compared only with random samples of $10^9$ alternative layouts).

The US system attains better connection-optimization than macaque or cat visual cortex, with no layouts better than actual found in a 1 billion sample. This may appear to vindicate the "invisible hand" of laissez-faire economics. However, the "Actual layout" curve departs markedly from the Size Law pattern; smaller subsets already attain perfect optimality--i.e., an optimality ratio of 0, with no alternative layouts better than the actual one. This breakdown suggests the macroeconomic networks are optimized locally, unlike the cortex (and some chip) networks. For calibration, the "Scrambled layout" (broken-line) curve, for the 15 U.S. states with their adjacencies randomly shuffled, shows the usual "flat" unoptimized pattern.

Previous | Next

**Table S6**. Component placement optimization: results summary. "Estimated Rank" designates proportion of all possible alternative layouts that are of lower connection-cost than the actual layout. Each layout is scored for violations of the Adjacency Rule. Size Law goodness of fit $r^2$ is for a model of the form of an inverse exponential function $y = ke^{-mx}$.

| | Number of Components | Estimated Rank | Size Law $r^2$ |
|---|---|---|---|
| **Neural Networks** | | | |
| Caenorhabditis elegans | 11 | $4.0\ 10^{-7}$ | 0.99 |
| Macaque Visual Cortex | 17 | $1.2\ 10^{-7}$ | 0.91 |
| Cat Visual Cortex | 15 | $7.2\ 10^{-6}$ | 0.94 |
| Cat Cortex Metamodules | 14 | $1.1\ 10^{-7}$ | 0.97 |
| Cat Cortex: | | | |
| Vis, Aud, Somato | 39 | [(3x) $10^{11}$]* | --- |
| **Non-Neural Networks** | | | |
| AMI49 Microchip | | | |
| Esbenson & Kuh Layout | 15 | $7.0\ 10^{-2}$ | 0.77 |
| Hong et al Layout | 15 | $3.3\ 10^{-1}$ | 0.69 |
| Lin & Chang Layout | 15 | $1.5\ 10^{-3}$ | 0.78 |
| Macroeconomic Networks | | | |
| USA Commodity-Flow | 15 | --- | --- |
| Europe Ex/Im | 8 | $4.0\ 10^{-4}$ | --- |

*In each of 3 separate replications, 100 billion randomly sampled layouts were tested without finding a better layout than the actual one.

**Table S7**. Connections vs adjacencies among network components: 2 x 2 contingency tables. For each neural system, the relationship is highly significant: $p < 0.0001$; $r > 0.30$. Connections and adjacencies to immediately contiguous edge-components are included. (Number of core components is given in parentheses.)

**Cortex Networks**

Macaque Visual Cortex (17)

| | Adj | NotAdj | Total | $X^2$ | *r* |
|---|---|---|---|---|---|
| Con | 38 | 82 | 120 | 30.6433 | 0.30801 |
| NotCon | 16 | 187 | 203 | | |
| Total | 54 | 269 | 323 | | |

Cat Visual Cortex (15)

| | Adj | NotAdj | Total | $X^2$ | *r* |
|---|---|---|---|---|---|
| Con | 40 | 86 | 126 | 40.0761 | 0.365496 |
| NotCon | 8 | 166 | 174 | | |
| Total | 48 | 252 | 300 | | |

Cat Metamodules (14)

| | Adj | NotAdj | Total | $X^2$ | *r* |
|---|---|---|---|---|---|
| Con | 44 | 90 | 134 | 37.09234 | 0.368605 |
| NotCon | 6 | 133 | 139 | | |
| Total | 50 | 223 | 273 | | |

Cat Vis/Aud/Som Cortex (39)

| | Adj | NotAdj | Total | $X^2$ | *r* |
|---|---|---|---|---|---|
| Con | 101 | 350 | 451 | 143.0408 | 0.333381 |
| NotCon | 18 | 818 | 836 | | |
| Total | 119 | 1168 | 1287 | | |

**Non-Neural Networks**

AMI49 Microchip

Esbensen & Kuh Layout (15)

| | Adj | NotAdj | Total | $X^2$ | *r* |
|---|---|---|---|---|---|
| Con | 17 | 95 | 112 | 0.62703 | 0.0409 |
| NotCon | 32 | 231 | 263 | | |
| Total | 49 | 326 | 375 | | |

Hong et al Layout (15)

| | Adj | NotAdj | Total | $X^2$ | *r* |
|---|---|---|---|---|---|
| Con | 14 | 86 | 100 | 0.00072 | 0.0016 |
| NoCon | 24 | 146 | 170 | | |

| | | | |
|---|---|---|---|
| Total | 38 | 232 | 270 |

Lin & Chang Layout (15)

| | Adj | NotAdj | Total | $X^2$ | $r$ |
|---|---|---|---|---|---|
| Con | 19 | 84 | 103 | 6.62842 | 0.1451 |
| NotCon | 18 | 194 | 212 | | |
| Total | 37 | 278 | 315 | | |

Macroeconomic Networks

USA Commodity-Flow (15) (@1500)

| | Adj | NotAdj | Total | $X^2$ | $r$ |
|---|---|---|---|---|---|
| Con | 47 | 137 | 184 | 29.4310924 | 0.274708 |
| NotCon | 12 | 194 | 206 | | |
| Total | 59 | 331 | 390 | | |

Europe Ex/Im (8) (@1250)

| | Adj | NotAdj | Total | $X^2$ | $r$ |
|---|---|---|---|---|---|
| Con | 23 | 36 | 59 | 8.06358 | 0.3098 |
| NotCon | 2 | 23 | 25 | | |
| Total | 25 | 59 | 84 | | |

Previous | Next

## References and Notes

1. Worm nervous system wiring data is as reported in: Cherniak, C. (1994) Component placement optimization in the brain. Journal of Neuroscience 14: 2418-2427 (1994). ( See also: Network Optimization in the Brain: Cerebral Cortex Layout [II: 2/2000] NIMH Grant Application, UMIACS Tech Report CS-TR-4525 . www.cs.umd.edu/Library/TRs/ )

2. Diagram adapted with revisions from: Felleman, D., and Van Essen, D. (1991) Distributed hierarchical processing in the primate cerebral cortex. Cerebral Cortex 1: 1-47. (Fig. 2, p. 4); Van Essen, D., et al (1990) Modular and hierarchical organization of extrastriate visual cortex in the macaque monkey. Cold Spring Harbor Symposia on Quantitative Biology LV: 679-696 (Fig. 6, p. 689). Areas MIP and MDP are included in PO.

3. Connections based upon: Scannell, J. (1997) Determining cortical landscapes. Nature 386: 452. www.psychology.ncl.ac.uk/jack/gyri.html; from Young, M. (1993) The organization of neural systems in the primate cerebral cortex. Proceedings of the Royal Society, B 252: 13-18. Adjacencies from Felleman and Van Essen (1991) (see note 2). Adjacencies do not include "diagonals", where only corners of two areas are contiguous (e.g., V3a and LIP in Fig. 2); similarly for all analyses below. (Because of incomplete information, the edgering has a gap at PS, 29, 30.)

4. Diagram based upon: Scannell, J., Blakemore, C., and Young, M. (1995) Analysis of connectivity in the cat cerebral cortex. Journal of Neuroscience 15: 1463-1483. (Fig. 1, p. 1466; with corrections.) Area SVA is included in 17, ALG in 19; DP in EPp & AI, V in VP & AII, SSF in EPp; a number of boundary indeterminacies remain unresolved.

5. Connections and adjacencies based upon Scannell et al (1995) (see note 4). Adjacencies do not include "diagonals", where only corners of two areas are contiguous.

6. Connection matrix of AMI49: Benchmark suite LayoutSynth92 1992 International Workshop on Layout Synthesis, North Carolina. www.cbl.ncsu.edu/pub/Benchmark_dirs/LayoutSynth92/bench90.tar.Z

7. Diagram based upon: Esbensen, H., and Kuh, E. A performance-driven IC/MCM placement algorithm featuring explicit design space exploration. ACM Trans. Design Automation of Electronic Systems, vol. 2, no. 1 (January 1997), p. 79, Figure 9(b). info.acm.org/todaes/V2N1/L134/paper.pdf

8. Diagram based upon: Hong, X., Huang, G., Cai, Y., Dong, S., Cheng, C., and Gu, J. Corner block list: An effective and efficient topological representation of non-slicing floorplan. Int. Conf. Computer-Aided Design, Nov.2000, pp. 8-12. www.cse.ucsc.edu/research/surf/GSRC/Papers/01a_2.pdf

9. Diagram based upon: Lin, J.-M. and Chang, Y.-W. TCG: A transitive closure graph based representation for non-slicing floorplans. In Proc. of ACM/IEEE Design Automation Conference

(DAC-2001), Las Vegas, NV, June 2001. Figure 6 (2).
http://cc.ee.ntu.edu.tw/~ywchang/Papers/tcg01.ps

10. State-to-State Commodity Flows: Commodity Flow Survey (1997). Bureau of Transportation Statistics, U.S. Department of Transportation. www.bts.gov/ntda/cfs/docs/cf97odv.html

11. International Trade by Commodity Statistics (1999). Organisation for Economic Co-operation and Development. www.oecd.org/xls/M00017000/M00017616.xls
(See also: Richardson, L. Statistics of Deadly Quarrels (Boxwood Press, Pittsburgh, 1960)) ch. 5.4.)

This work was supported by NIMH grant MH49867. NCI generously made available supercomputers at their Advanced Biomedical Computing Center. We thank Richard Kissh for parallel supercomputer software engineering. We are also grateful for assistance of Eric Celarier, Jarrett Rosenberg, Thomas Schaefer, and Corey Washington.

Previous | Home